Reducing Waste Heat to the Minimum: Thermodynamic assessment of the M-Power cycle concept applied to micro Gas Turbines

Ward De Paepe[a,*], Alessio Pappa[a], Marina Montero Carrero[b], Laurent Bricteux[a], Francesco Contino[c]

[a] *University of Mons (UMONS), Dept. of Mechanical Engineering, Rue de l'Epargne 56, 7000 Mons, Belgium*
[b] *Vrije Universiteit Brussel (VUB), BURN joint research group, pleinlaan 2, 1050 Brussels, Belgium*
[c] *Université catholique de Louvain (UCLOUVAIN), Institute of Mechanics, Materials and Civil Engineering (IMMC), Place du Levant 2, 1348 Louvain-la-Neuve, Belgium*

Abstract

To fully embrace its opportunities in future decentralized power production, the current mGT has to become more flexible in terms of operation, i.e. decoupling heat and power production. Cycle humidification during periods with low heat demand is a possible route to handle this issue. Indeed, cycle humidification has already been proven to increase the mGT electrical efficiency. Nevertheless, even when applying the most advanced humidified cycle concept, i.e. the REgenerative EVAPoration cycle, the electrical performance increase remains rather limited. In this perspective, the more recent Maisotsenko (or M-power) cycle concept offers a larger potential for humidification, even though its potential was only proven on large-scale gas turbine

*Corresponding author
Email address: ward.depaepe@umons.ac.be (Ward De Paepe)
URL: http://staff.umons.ac.be/Ward.DEPAEPE/ (Ward De Paepe)

cycles and never applied to the smaller mGT scale.

In this paper, the concept of this M-power cycle is applied to a 100 kW_e mGT (Turbec T100) to assess its performance, using Aspen Plus® simulations. Moreover, the impact of various inputs, component performance and control parameters is studied using a sensitivity analysis. The numerical results highlight that the M-power cycle has the highest waste heat recovery and thus the highest electric efficiency (up to 147 kW_e electric power output with an electric efficiency of 42.1 % at constant rotational speed and 41.1%, corresponding to an 8.3%point absolute increase, at constant power output). Moreover, this cycle concept allows to approach the thermodynamic limit for cycle humidification. Indeed, a large exergy destruction is avoided by not going for direct water injection, but rather using a gradual injection and evaporation. Additionally, from a technological point of view, the M-power cycle is also preferable for the small-scale mGT. Indeed, in the M-power cycle, saturation tower, aftercooler, recuperator and economizer are combined in one single component, significantly reducing the complexity of the cycle. The main limitation is the saturator, that requires a wet bulb effectiveness of up to 98 % to achieve the simulated performance, which can be technological very challenging.

Keywords: micro Gas Turbine (mGT), cycle humidification, waste heat recovery, REVAP, M-power cycle

1. Introduction

The massive deployment of Renewable Energy (RE) in electricity production has significantly changed the energy landscape over the last 10 years.

The highly intermittent nature of RE is putting a severe constraint on the stability of the electricity grid, requiring more flexible operation from the classical thermal power production units [1]. This has led to a shift from large-scale centralized to small-scale decentralized production, possibly in combination with heat production (Combined Heat and Power (CHP)). In this perspective, micro Gas Turbines (mGTs) offer great potential, since they have a higher flexibility as a result of their smaller size [2]. However, given their relatively low electric efficiency, these units are still only profitable when used in CHP applications with a sufficiently high heat demand [3]. Cycle humidification offers a solution to increase electric efficiency in moments of low heat demand, which has already been proven economically viable [4, 5].

Cycle humidification was first proposed on large-scale Gas Turbines (GTs), initially to reduce NO_x emissions and later to increase power production and for overall cycle performance improvement [6]. In their review paper, Jonsson and Yan divided all existing humidified GT cycles into 3 categories, including: injection of liquid water that will fully evaporate, injection of steam, and injection of liquid water in a saturation tower with a water recovery loop [6]. From these different cycles, the latter option, using a saturation tower and water recovery loop, i.e. the Humid Air Turbine (HAT) cycle first proposed by Rao [7], was found to be the best performing cycle. Following up on the HAT cycle development, several, more advanced variants of this cycle, like the Evaporative Gas Turbine (EvGT) [8], the Cascaded Humidified Advanced Turbine (CHAT) [9] or TOP Humid Air Turbine (TOPHAT®) [10], have been proposed. Finally, using second law analysis, Bram et al. were able to develop an alternative for the HAT cycle, the REgenerative EVAPoration

(REVAP®) cycle [11]. This cycle achieves similar performance as the HAT cycle, without requiring the installation of a saturation tower [12].

Several of the proposed advanced humidified GT cycles have been applied at the smaller mGT scale in the past, going from very simple layouts, i.e. direct injection of (preheated) water or steam in the compressor outlet, to more advanced and complex cycles, like the micro Humid AirTurbine (mHAT), mHAT+ [13] (which is based on the original HAT cycle) or the REVAP® cycle [14]. The application of several more complex cycles, like the CHAT and TOPHAT® is not possible on the mGT scale, since there is no option for intercooling, given that, so far, mGTs only work with one compressor stage. Depending on the complexity of the cycle, only numerical work is presented so far (REVAP®), while for the simplest cycles (water/steam injection and mHAT cycle), their potential has already been proven experimentally. An overview of all works performed on mGT cycle humidification can be found in [15].

An in-depth thermodynamic analysis of these cycles was performed by the authors of this paper on a Turbec T100 mGT, showing that the REVAP® cycle with water preheat has the highest potential of all humidified cycles (injection of 69.5 g/s of water leads to a net electrical power output increase of 21.7 kW_e and an absolute efficiency increase of 4.58 %point at constant rotational speed), followed by the direct water injection cycle, with feedwater preheat and 2-phase flow entering the recuperator (maximal injection of 58 g/s, leading to 18.0 kW_e extra production with an absolute efficiency increase of 3.84 %point at constant rotational speed [14]). The mHAT cycle, which was identified as the best compromise between cycle performance and

complexity [16], only presents a limited water introduction of 56.6 g/s leading to a moderate performance improvement of 17.5 kW_e and 3.75%point efficiency increase at constant rotational speed [14].

Nonetheless, none of these cycles can approach the theoretical maximum waste heat recovery through cycle humidification: injection of 155 g/s leads to a 47.4 kW_e power output and 9.5 %point absolute efficiency increase [17], which was found through a second law analysis [12]. The major limitation to approach this maximum was the inability of the proposed cycles to recover the large amount of evaporation enthalpy from the flue gases at low temperature due to the condensation of the water. From this point-of-view, the Maisotsenko, or M-power, cycle might offer a solution [18]. This M-cycle is a promising air cooling technique that can reduce the temperature of the air flow until its dew point, which is not possible either in direct contact techniques or former indirect evaporative methods. This cooling method can be applied on GTs, but also on air conditioning systems, cooling towers and electronic cooling [19]. This cycle combines the aftercooling as proposed in the mHAT+ and REVAP® cycles, creating a low temperature cold stream to recover more waste heat, with the evaporation process at variable temperature as can be found in the mHAT cycle, enabling water introduction without excessive exergy destruction.

The M-power cycle was first proposed by Gillan and Maisotsenko in 2003 for application on large-scale GT cycles [18]. According to its developers, the M-power cycle combines the thermodynamic processes of heat exchange and evaporative cooling in an unique indirect evaporative cooler, allowing to approach the dew point temperature of the working fluid [20]. By com-

bining the heat exchange and evaporative cooling in one single component, the cycle layout of the M-power cycle is simpler compared to alternative advanced humidified GT cycles, like the previously mentioned EvGT [8], HAT [7], CHAT [9], TOPHAT® [10] or REVAP® [11]. According to Gillan and Maisotsenko, an overall thermal efficiency of 60% could be reached [18].

Since the first presentation of the M-power cycle, several numerical studies have been presented on its potential in large-scale GT cycles [21]. Reyzin confirmed the M-cycle unique heat recovery capabilities and even presented that an 80% thermodynamic efficiency for a GT utilizing the M-power cycle could be within reach [21]. More recently, Galadda and co-authors have presented several works on the M-power cycle [22–25]. An initial analysis focused on the use of the M-coolers in a GT to improve the performance, highlighted the large savings potential if this inlet air cooling technique was applied on a 50 MW_e GT power plant [23]. They also indicated that the efficiency of the cycle mainly depends on the effectiveness of the cooling and the saturation processes [22]. Finally, they also presented two cases of the M-power cycle applied again on large-scale GTs, focusing on the development of a detailed model of the air saturator. The authors indicated that the efficiency could be improved by 3.7 %point if the cycle was used as bottoming cycle of a classical GT [25] and even 7 %point, while augmenting the net performance by 44%, when implementing it directly in the GT cycle [24]. Additionally, Tariq and Sheikh evaluated the concept of the Maisotsenko humid air bottoming cycle for waste heat recovery unit for GT topping cycle. They indicated that the proposed configuration gives maximum work output (58 MW_e) and efficiency (34%) at an air saturator exit relative humidity

of 70% [26]. Most recently, Zhu et al. analyzed the performance of the M-power saturator and compared it with a traditional evaporator-cooler, proving again the superiority of the M-power cycle [27]. However, despite showing to be theoretically the best option for humidification of large-scale GT cycles, the concept has not yet been validated experimentally, nor has it been implemented at the smaller mGT scale.

In this paper, we present therefore a global thermodynamic analysis of the performance and potential of the M-power cycle on mGT scale. To show the potential of this cycle, an experimentally validated numerical model of a typical mGT, being the Turbec T100, is converted into the M-power cycle by implementing the specific saturation module. The impact of the performance of the specific saturator on the global cycle performance is assessed using a sensitivity analysis. Moreover, in an attempt to better understand the high performance of the M-power cycle, an extensive exergy analysis was performed, using a Grassmann diagram. Finally, recommendations concerning future M-power cycle development on the mGT are formulated.

2. Methodology

The M-power cycle can be recognized by the very specific saturator module (Figure 1), that is replacing the classical recuperator from the mGT, operating according the recuperated Brayton cycle. This component combines the actions of the aftercooler, evaporator and recuperator, as can be found in the more traditional humidified GT cycles, e.g. the HAT or REVAP®. When applying this concept to the mGT, compressed air, coming from the variable speed radial compressor (2), is first cooled down in the lower part of the sat-

urator (3). This happens thanks to the evaporation of injected water (11), introduced in the returning compressed air (typically a third of the total compressed air stream). This stream leaves the lower part of the saturator module fully saturated (4). The remaining cooled compressed air enters the upper part of the saturator (3), where it is humidified by water injection (10). In this section, the liquid water evaporates and the stream is heated, using heat coming from the flue gases. After bringing both streams together (4 and 5), the humidified compressed air is heated further in the end-part of the upper section of the saturator (6). Once leaving the saturator, the working fluid completes the classical route of the recuperated Brayton cycle: passing through the combustion chamber to increase the temperature (7), then expanding over the turbine to provide power to drive compressor and generator for electric power production (8) and finally providing the necessary heat to evaporate and preheat the humidified compressed air when passing through the upper part of the saturator (9).

The main advantage of the M-Power saturator is that, by introducing water in both the cold side of the lower part of the saturator (11) as well as in the cold side of the upper part of the saturator (10), a maximal amount of heat can be recovered. By injecting in the lower part, heat can be recovered from the incoming compressed air: lowering the temperature of the inlet of the upper part (3) and thus enabling for more waste heat recovery from the flue gasses. Additionally, the injection in the cold side of the upper part (10), together with the lower inlet temperature, allows for even more waste heat recovery from the flue gases, leading to optimal performance.

To assess the potential of this M-power cycle at mGT scale, the Turbec

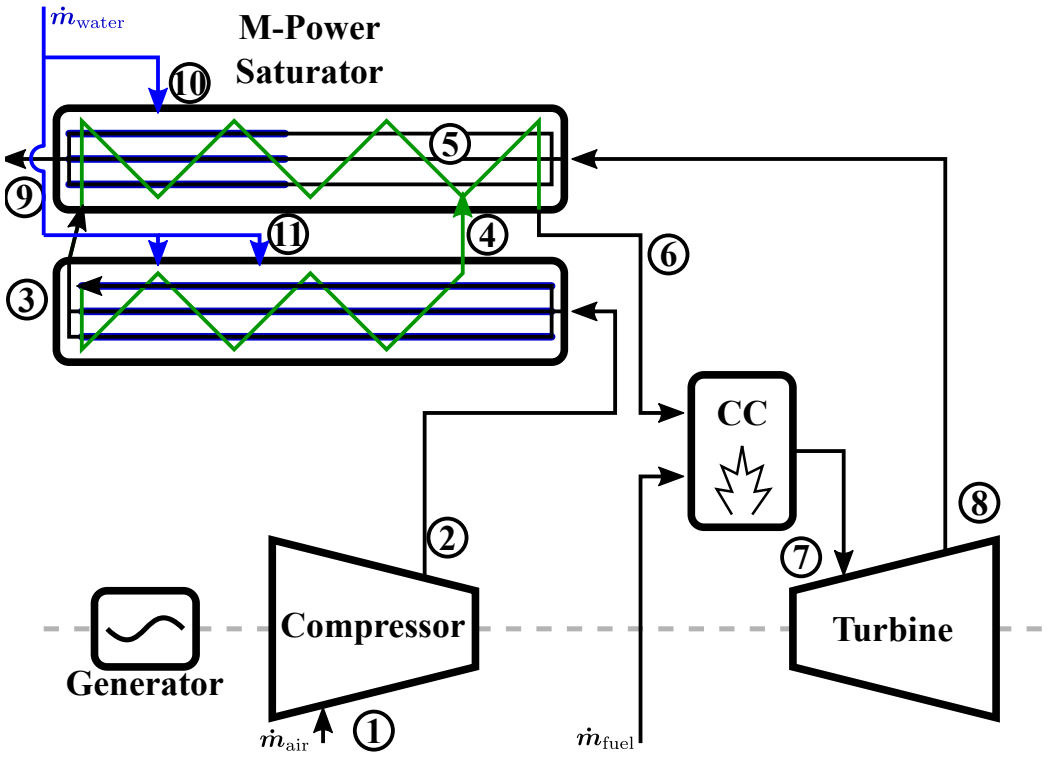

(a) M-power cycle applied to the mGT

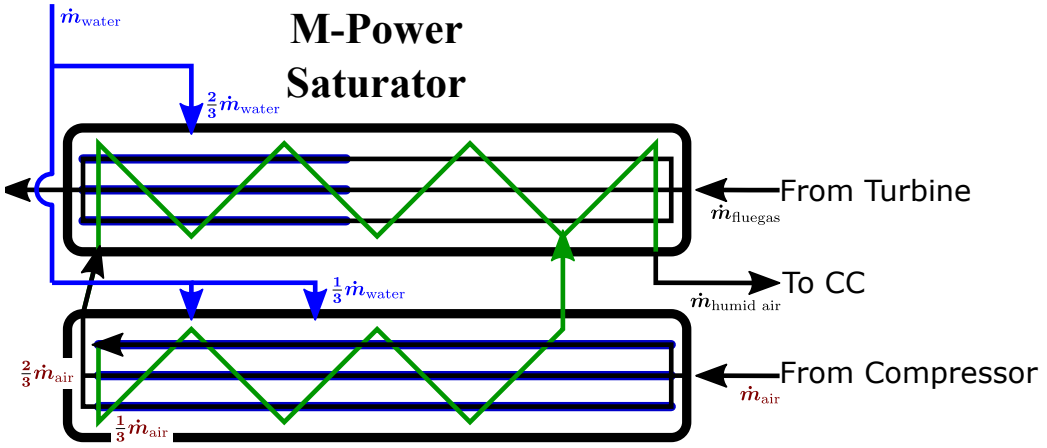

(b) Zoom of the M-power saturator, including split fractions

Figure 1: The M-power cycle applied on the mGT (a) showing the integration of the M-Power saturator in the cycle (b), replacing the recuperator from the classical recuperated Brayton cycle.

T100, a classical recuperated mGT, was selected. A previously developed and experimentally validated Aspen Plus model of the mGT [28, 29] was adapted by integrating the typical M-power saturator between compressor outlet and combustion chamber inlet. To allow for a correct comparison with other humidified mGT cycles, the remaining components, being compressor, turbine, combustion chamber and electric generator, were simulated as discussed in [14] and briefly described below.

To determine the compressor outlet pressure and isentropic efficiency, the actual compressor map of the Turbec T100 was used in the simulations (see Figure 6) [30], while the turbine was assumed to be choked: the choking value is corrected for the changing turbine flow composition using following equation [31]:

$$\frac{\dot{m}_{\text{turb}}\sqrt{\text{TIT}}}{\text{TIP}} = A\sqrt{\frac{k_{\text{turb}}}{R}\left(\frac{2}{k_{\text{turb}}+1}\right)^{\frac{k_{\text{turb}}+1}{k_{\text{turb}}-1}}} = cte \tag{1}$$

where k_{turb} corresponds to the heat capacity ratio of the turbine working fluid, R is the universal gas constant and A is the cross section area of the turbine. In the Aspen Plus® model, this choking value was kept constant by implementing a control loop that alters the compressor inlet air mass flow rate. The turbine isentropic efficiency, on the other hand, was corrected for the changing working fluid based on suggestions of Parente et al. [13].

$$\frac{\eta_{\text{is}}}{\eta_{\text{is}}^{*}} = \frac{k-1}{k^{*}-1}\sqrt{\frac{k^{*}+1}{k+1}\frac{1-1/\pi^{\gamma^{*}}}{1-1/\pi^{\gamma}}}. \tag{2}$$

In Equation 2, the apex (*) refers to the properties at standard air composition, while γ is defined as $(k-1)/k$. Depending on the selected operating regime, the mGT operates at constant rotational speed and thus variable

power output or at constant generated electrical power by varying the rotational speed. For correct comparison, similar allowed maximal pressure and heat losses as used in [14] were also included in the different components. These losses would then be used in a later phase as design conditions for the heat exchanger/saturator. Moreover, similar control loops, allowing to operate at constant Turbine Inlet Temperature (TIT) of 950°C and rotational speed or power output have been implemented. To calculate the physical properties, the *UNIFAQ* method was used. All the used parameters in the Aspen Plus® model are presented in Table 1 (for a full discussion on the implementation and selection of the values, we refer the reader to [14]). Finally, as previously indicated by the authors, the response of the turbomachinery to the addition of water is independent of the water introduction method, once this occurs behind the compressor. Only the amount of introduced water will determine the off-design behavior, as was shown numerically [14] and validated experimentally [32]. Hence we can assume that, despite no experimental validation of the Aspen Plus® M-power cycle model is possible at this stage, the turbo-machinery off-design behavior, and in an extend the global M-power cycle concept applied to mGTs, is correctly captured.

To simulate the specific saturator model in Aspen Plus®, the methodology as proposed by Saghafifar and Gadalla was implemented [24]. Although the humidification of the compressed air occurs using an excess of water, Saghafifar and Gadalla argued that the saturator could be reduced to a simple direct water injection cycle, expressing global energy balances. In this context, the specific saturator was replaced by a series of heaters/coolers and water injectors in the Aspen Plus® model developed for this paper (as can

Table 1: Boundary conditions used for the M-Power mGT cycle development.

Compressor	
Inlet air temperature	15°C
Inlet air pressure	1.013 bar
Inlet air humidity	60%
Rotational Speed	67320 rpm/variable[1]
Mechanical efficiency	99%
Combustion Chamber	
Combustor design pressure loss	5%
Combustor design heat loss	10 kW_{th}
Turbine	
Turbine back pressure	40 mbar
Turbine Inlet Temperature (TIT)	950°C
Mechanical efficiency	99%
Heat exchanger network	
Cold side design pressure loss	3%
Hot side design pressure loss	40 mbar
Water injection design pressure loss	0.5%
Feed water temperature	15°C
General	
Fuel (methane) Lower Heating Value	50 MJ/kg
Combined power electronics efficiency	94%
Produced electrical power	variable/100 kW_e[2]

[1]Depending on the operation mode, constant power output or constant rotational speed, the rotational speed is variable to control power or kept constant by the control system.

[2]Depending on the operation mode, constant power output or constant rotational speed, the rotational speed is variable to control power or kept constant by the control system.

be seen in the Aspen Plus® flowsheet, Figure 2), since no such specific saturator/heat exchanger block is available. Moreover, by not using a series of classical heat exchanger blocks (*HeatX*-block), but rather using the simpler variant, the heater block (*Heater*-block), the calculation time, given the large number of convergences loops, could be reduced significantly. Additionally, the use of simple heater blocks also led to a more stable simulation model, especially when approaching the upper limit for water introduction.

The lower part of the saturator was replaced by 1 heater and 1 cooler (*SLOWCOLD* and *SLOWHOT* from Figure 2). The incoming compressed air is cooled down to a specified temperature, determined by the following equation (subscripts correspond to states from Figure 1):

$$T_3 = T_2 - \epsilon_{\text{dew}} \left(T_2 - T_{dew,2} \right) \tag{3}$$

where T_2 is the incoming air temperature of the compressed air; $T_{\text{dew},2}$ the dewpoint temperature of this compressed air stream; and T_3 the temperature of the compressed air being cooled down. ϵ_{dew} represents the dew point effectiveness of the evaporation process that occurs in the cold side of the lower part of the saturator and is typically taken equal to 0.8 [20]. Indeed, in this paper, we aim at assessing the potential of the M-power cycle for mGT. So rather than simulating the performance of a real application, the dew point effectiveness ϵ_{dew} was kept constant at a typical value found in literature. Once the potential is assessed and the optimal cycle is identified, a real design proposal needs to be formulated for the M-power cycle, with a dew point effectiveness of $\epsilon_{\text{dew}} = 0.8$ as design condition.

The extracted heat from the hot stream is used to evaporate part of the injected water in the compressed air stream (typically one third of the to-

tal air stream going through the cycle) and heat the 2-phase flow mixture. The outgoing humidified air stream of the cold side of the lower part of the saturator (stream 4 from Figure 1) is expected to be fully saturated, with a remaining liquid water fraction. As mentioned before, no actual heat exchangers, but rather simple coolers/heaters have been used for the simulation of the heat exchange. This means that Aspen Plus® will not detect any violation of the second law. Therefore, any solution leading to a negative or smaller than 15°C hot pinch on the lower part of the saturator (temperature difference between T_2 and T_4) was found not feasible by the authors and is therefore discarded.

The upper part of the saturator is simulated using 2 heaters (cold side, *STOPCOLD* and *SEND* from Figure 2) and 1 cooler (hot side, *STOPHOT* from Figure 2). Before entering the upper part, water is injected in the cold compressed air (same water fraction as in the cold stream entering the cold side of the lower section of the saturator). Using the heat from the exhaust gases, the water is fully evaporated in the first heater (vapor fraction equal to 1). Afterward, both humidified compressed air streams (streams (4) and (5) from Figure 1) are mixed and heated further in the second heater, using the remainder of the heat from the flue gases. The total amount of available heat is determined by the temperature of the flue gases. The cooler cools down the flue gases to a specific temperature, as could be found by using following expression (subscripts correspond to states from Figure 1):

$$T_9 = T_8 - \epsilon_{\mathrm{WB}} \left(T_8 - T_{\mathrm{WB},3} \right) \tag{4}$$

where T_8 is the incoming temperature of the flue gases (which is also known as Turbine Outlet Temperature (TOT)); T_9 the outgoing temperature; $T_{\mathrm{WB},3}$

the wet bulb temperature of the compressed air; and ϵ_{WB} the wet bulb temperature effectiveness, typically taken equal to 0.9 [20], for the same reason as mentioned when discussing the constant ϵ_{dew}. Since Aspen Plus® does not calculate wet bulb temperature, hence $T_{\mathrm{WB},3}$ was found using the humid air enthalpy from point 3 together with the calculation of the absolute humidity using the saturation and actual pressure. By moving along an iso-enthalpic line towards the saturation curve, finally, the wet bulb temperature could be found. The outgoing temperature of the humidified compressed air (T_6) is calculated using the global energy balance, knowing the total available and exchanged heat, given that the temperature of the outgoing flue gases is fixed (T_9, see Equation 4). However, since the cold side can never exit the saturator outlet at a temperature superior to the hot side inlet temperature, a minimal temperature difference should be respected. Saghafifar and Gadalla proposed 15°C [24]; however, in our opinion this value is too small for an actual application. Indeed, the smaller the pinch, the larger the actual heat exchanger needs to be to achieve this low pinch. Therefore, for the M-power cycle applied on the mGT, a more conservative 50°C temperature difference was used on the hot side of the recuperator [14], which corresponds to a typical pinch of a gas-gas heat exchanger in mGTs. Moreover, using this pinch allows for comparison between the results presented in this paper with previous work [14], where a similar hot pinch was used for the heat exchanger network.

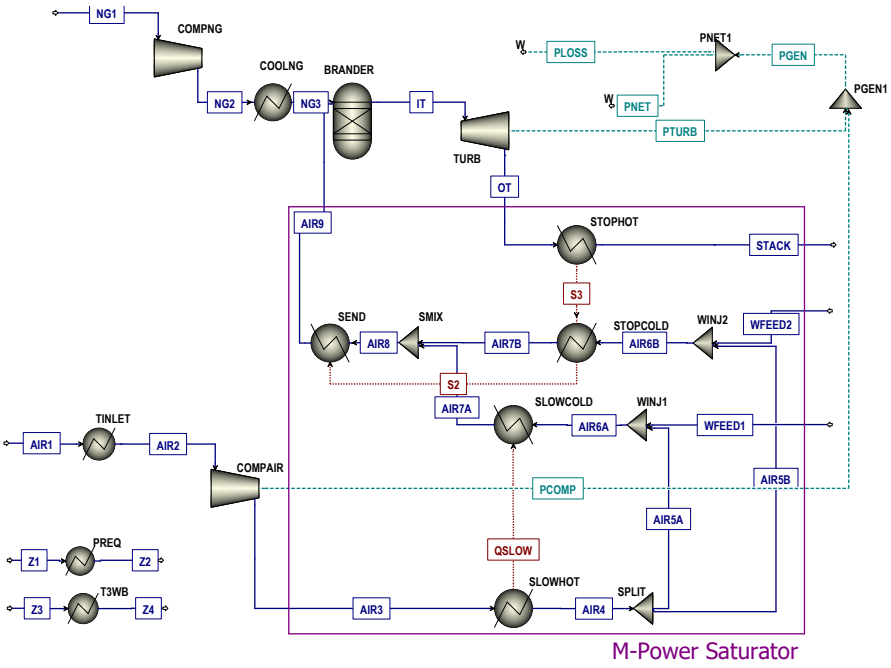

Figure 2: Aspen Plus® flowsheet of the M-Power cycle applied to the mGT with the specific M-power saturator (purple box).

3. Results

In this section, first the global performance of the M-power cycle applied at mGT scale is assessed and optimized, using Aspen Plus® simulations performed at constant rotational speed and power output, followed by a discussion on the technical impact/limitations of water injection on the mGT. In a third section, by means of a sensitivity analysis, the impact of the various parameters on the global cycle performance is identified. Finally, an exergy analysis is presented using a Grassmann diagram to identify the main advantages of the M-power cycle concept.

3.1. General performance assessment and optimization

First, the impact of changing the amount of injected water on the global cycle performance of the M-power cycle applied on the mGT was assessed at constant rotational speed (67320 rpm) and using the boundary conditions set in Table 1. Moreover, the effectiveness of both the lower and upper parts were kept constant, as discussed before, at specific realistic design specifications ($\epsilon_{\text{dew}} = 0.8$ and $\epsilon_{\text{WB}} = 0.9$). Unlike previous humidified cycle simulations where the optimal/maximal amount of injected water could be found by imposing minimal pinches on the different heat exchangers [14], here, it is not possible to fix the boundary conditions such that automatically the maximal possible water introduction amount could be found. Indeed, in [14], the heat exchange network consisted only out of indirect heat exchangers and a water injection point. By setting the pinch for each individual heat exchanger, automatically their heat flux is determined. Adding on top of this a hot pinch for the global heat exchanger network, fixes automatically the amount

of water that must be injected (the only remaining degree of freedom), hence, the system is fully determined. For the M-power cycle, on the one hand, only the heat recovered from the flue gases is set (Equation 4), as well as the heat recovery in the lower part (Equation 3). Additionally, the first law should be respected (conservation of energy). On the other hand, the M-power cycle can be seen as a combination of 3 heat exchangers with also water injection, meaning that for each of these heat exchangers, the heat flux must be set/calculated, together with the amount of introduced water, leaving thus 4 degrees of freedom. Since only 3 equations are set, one degree of freedom is left, allowing to work with a variable amount of injected water. Implementing an extra intermediate pinch in the system will determine automatically the amount of water. This is not possible in the M-power cycle, since it consists in a simultaneous heat and mass transfer process. Hence, rather than fixing a temperature difference (as is the case in indirect heat exchangers), one should fix the humid air enthalpy difference, however, this is neither possible in Aspen Plus®. Therefore, the amount of injected water was gradually increased, dividing the water as discussed before: one third in the lower part of the saturator (point 11 from Figure 1) and two thirds in the upper part of the saturator (point 12 from Figure 1).

It is clear from the Aspen Plus® simulation results that increasing the amount of injected water will indeed increase the electric power output of the cycle (Figure 3 (a), $\epsilon_{\mathrm{WB}} = 0.9$, green curves); however, the efficiency is decreasing (Figure 3 (b)). The increasing power output can be explained by the higher water injection in combination with the choking condition on the turbine. When increasing the amount of injected water, part of the air

is replaced by water, as a result of the turbine choking. Indeed, increasing water injection forces the compressor to shift towards lower mass flow rates (in constant rotational speed mode) or lower mass flow rates and rotational speed (constant power output mode), leading in both cases to a surge margin reduction (see subsection 3.2). Since in both cases, the compressor air mass flow rate is reduced, the compressor work will reduce significantly (while the turbine work slightly increases due to the increasing heat capacity of the working fluid), leading to an increased net power available on the shaft for conversion in electric power. At the same time, the effectiveness of the saturator is fixed, meaning that the final stack temperature of the flue gases does not change significantly for increasing water injection flow rate. A large amount of heat is still available in these flue gases as evaporation heat. All of this heat is lost (high stack temperature of 107°C, Figure 4), leading to a significant electric efficiency reduction (even below the electrical efficiency of the dry mGT, 32.8%[1], see Table 2).

Simulation results also indicated, that, for the used boundary conditions, there is not only an upper limit for maximal water injection in the M-power cycle applied on the mGT but there is also a lower limit for water injection (Figure 3). When using a fixed wet bulb (ϵ_{WB}) and dew point (ϵ_{dew}) effectiveness for the lower and upper part of the saturator respectively, injecting less than 33 g/s leads to a violation of the second law at the hot side of the

[1]The Turbec T100 has a nominal 30% electric efficiency according to the manufacturer [33]. However, for correct comparison, the same boundary conditions as applied on the humid cycles have been applied on the dry cycle (Table 1), leading to a slightly higher efficiency of 32.8%. A similar approach was also applied in previous work [14]

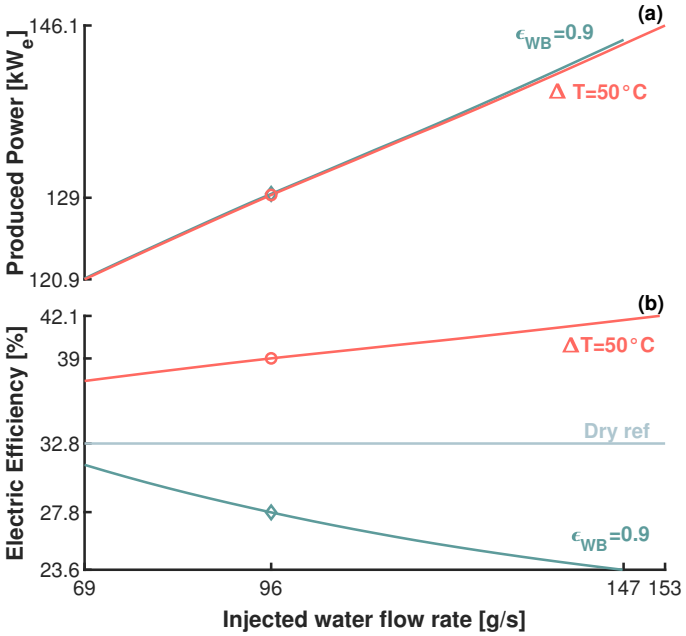

Figure 3: Performance results of the M-power cycle, using different assumptions on the M-power saturator performance, indicate that by maximizing the waste heat recovery only ($\Delta T = 50°C$ case), both electric power output (a) and efficiency (b) can be improved.

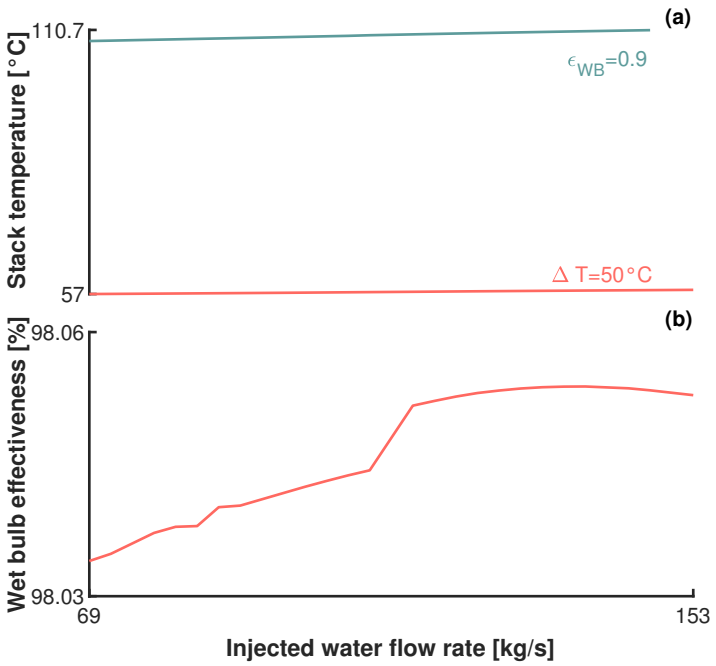

Figure 4: Performance of the M-power cycle, using different assumptions on the M-power saturator performance, indicate that only by maximizing the waste heat recovery and thus reducing the stack temperature (a), both electric efficiency and power output can be improved (case $\Delta T = 50°C$). However, this requires a very high wet bulb effectiveness ϵ_{WB} of over 98% (b).

upper part of the saturator, where the temperature of the cold humidified stream exits the heat exchanger above the temperature of the hot flue gases entering the saturation tower (to respect the 50°C temperature difference, at least 51 g/s should be injected in the cycle). However, to respect a minimal pinch of 15°C at the hot side of the lower part of the saturator, at least 69 g/s of water needs to be injected. The main reason for the relative high minimal injection is the fixed split of air mass flow rate in the cycle. Indeed, only a third of the air mass flow rate returns in the lower part, being heated by the full hot compressed air flow coming from the compressor. Only by increasing the amount of water, the temperature increase of the cold fluid can be limited to end up below the hot outlet temperature. For the first part of the upper section (between point 3 and 5 from Figure 1) in none of the simulations, a violation of the second law was found, always leaving a hot pinch above 15°C.

The found lower limit for water injection in the simulations presented in this paper is a result of the specific way the heat exchange in the upper and lower part of the heat exchanger is calculated, using Equation 3 and Equation 4 with fixed wet bulb ϵ_{WB} and dew point ϵ_{dew} effectiveness. Using this approach, the heat extracted from the hot stream is calculated, without verifying if the cold stream can actually accept this, respecting the second law. Although the used values for $\epsilon_{\mathrm{WB}} = 0.9$ and $\epsilon_{\mathrm{dew}} = 0.8$ being typical values taken from literature [20], they still assume that there is a certain heat exchanger/evaporation process ongoing in the M-power saturator. When a too little amount of water is injected, the M-power saturator will behave more like a classical indirect heat exchanger, rather than an evaporator and thus

these values are no longer valid and one should not work with wet bulb and dew point effectiveness, but rather with actual effectiveness (based on actual temperatures) to calculate this heat exchange. A possible workaround would be, that once a second law violation is noticed, the effectiveness is reduced in the simulation model and hence allowing to continue the simulations. However, since in this paper, we aimed at maximizing the waste heat recovery, which can only be done by maximizing the water injection, hence there was little interest in implementing this in the simulation model.

The upper limit for water injection was found at 147 g/s when assuming $\epsilon_{\mathrm{WB}} = 0.9$. Injecting more water will lead to a compressor surge (for full discussion, we refer to subsection 3.2). This maximal water amount is lower than the maximal amount found using the second law analysis (155 g/s, [14]). The reason can be found in the choking of the turbine together with the large difference in efficiency between the $\epsilon_{\mathrm{WB}} = 0.9$ case (23.6%) and the second law analysis (42.3%). Since the turbine is choked, the total mass flow rate in the cycle remains constant. Indeed, TIT remains constant through the action of the control system, as well as the outlet pressure (see Figure 6). Additionally, the choking constant itself is hardly changing due to the altering composition of the flue gases (injected amount of water is still limited). As can be concluded from Equation 1, the mass flow rate going through the turbine, being the sum of the compressor air mass flow rate, the injected amount of water and finally the fuel mass flow rate, remains constant. Since in the second law analysis, more waste heat is recovered and thus less fuel is needed, more water can be introduced before compressor surge is reached, explaining this small difference. Finally, in previous section, it was mentioned that the

humid compressed air is leaving the lower part (point 4 from Figure 1) of the saturator fully saturated with still some liquid water present. However, only starting from an injection of 96 g/s (diamond symbols indicated in Figure 3) the air is fully saturated and thus having a liquid fraction before entering the top part of the saturator.

These first results clearly highlight that higher injection rates lead to higher power outputs (Figure 3); however, these higher injection rates also need more waste heat recovery. Especially stack temperature should be lowered (now 107°C over the full injection range, Figure 4), dropping below the dew point of the flue gases, which enables the recovery of the available heat of evaporation of the water in the flue gases. In a second simulation, rather than fixing the flue gas outlet temperature of the saturator by assuming a given design wet bulb effectiveness ϵ_{WB}, the hot side temperature difference was fixed at 50°C (see Figure 3, $\Delta T = 50°C$ red curves). This 50°C temperature difference on the saturator hot side was, as mentioned before, assessed to be the minimal pinch that should be respected to allow for realistic heat exchanger performance, limiting their effectiveness, still leading to realistic design specifications. This simulation allows to push the heat exchange to a maximum, still respecting the second law, finally presenting the real potential of the M-power cycle for mGT applications.

Allowing for more waste heat recovery leads to a significant lower stack temperature (Figure 4 (a)), which leads together with the increasing electrical power output to a significant higher electric efficiency with increasing introduced water amounts (Figure 3 (b)). The electrical power output on the other hand is only dependent on the amount of injected water and not on the

waste heat recovery (Figure 3 (a)). Indeed, power production only depends on TIT, turbine inlet pressure and mass flow rate. Since the mGT operates at constant rotational speed and the turbine is choked, for a given injected water flow rate, turbine inlet pressure and mass flow rate remain constant, independent of the waste heat recovery. In addition, TIT is kept constant by the mGT control system. This indicated that all parameters having an influence on the electrical power output remain constant for a given fixed amount of injected water. Therefore, this power output is thus independent of the amount of waste heat recovered.

For all water injection flow rates respecting the second law (hot pinch of the saturator of at least 50°C and of the lower part of the saturator of 15°C), the flue gases reach their condensation point (57°C) and thus extra evaporation heat is released (Figure 4). When performing direct injection in a similar configuration (REVAP® cycle), only a maximal water amount of 69.5 g/s could be injected, before a cross in the temperature profiles was detected in the upper part of the heat exchanger network [14], only recovering a small fraction of the latent heat. Since the M-power cycle uses saturation, higher performances are possible. This can be seen in the maximal injection amount of 153 g/s for an electric efficiency of 42.1% (9.3%point absolute increase), which is equal to the thermodynamic limit found using second law analysis (small difference due to the step of 3 g/s used for simulations) [14]. However, to achieve this low stack temperature and corresponding latent heat recuperation, a dew point effectiveness above 98% (even up to 98.1%) is necessary (Figure 4 (b)). This may cause some technical difficulties.

Such a high wet bulb effectiveness can indeed be technologically challeng-

ing, since it requires a large contact area for heat exchange in the M-power saturator. Especially designing a saturator of such a large size, respecting the maximal pressure loss (5%, Table 1), can be difficult or even impossible. In that case, a slightly higher pressure loss can be accepted, leading to a minor efficiency penalty. Nevertheless, this penalty will be limited, still leading to an improved performance of the M-power cycle compared to the dry and any other humidified mGT cycle. Finally, this larger area will also lead to an increased size and linked capital cost of this saturator. The larger volume can possibly lead to instabilities on the compressor level when performing load changes [34], while the higher cost can make the cycle concept economically not profitable [4]. Dynamic cycle behaviour assessment, as well as a full thermo-economic analysis of the M-power cycle are outside the scope of this paper, but will be topic of our future work.

Finally, a full overview of the thermodynamic conditions of the M-power cycle applied on the T100 mGT at each stage of the cycle is presented (Table 2) for operation at the maximal water injection amount at constant rotational speed for the 2 considered case: using constant wet bulb effectiveness or constant hot pinch. The performance of the compressor is only affected by the amount of water and not the used assumption for the saturator: both cases present very similar compressor performance. Additionally, the performance of the lower part of the saturator is also very similar, due to the use of the same ϵ_{dew} in both cases. The main difference is found in the upper part, where there is a significant difference in cold side outlet temperature T_6 (381.3°C versus 646.3°C). The lower temperature in the constant wet bulb case results in a higher stack temperature T_9, indicating that less heat is

recovered. Hence, more fuel needs to be added in the combustion chamber (100% increase compared to the dry reference case) to achieve the same combustor outlet temperature, explaining the very low electric efficiency. The requested fuel flow rate is even higher than the amount that can be delivered by the current fuel compressor (9.9 g/s [35]), requiring thus a larger fuel compressor. Since the mGT is operated at constant TIT, the turbine performance is also very similar in both cases. This similar turbine performance, together with the same compressor performance, leads finally to the same electrical power output in both cases.

Similar observations as for the operation at constant rotational speed can be made at constant power output for the behavior of the M-power cycle electric performance (Table 2 and Figure 5). Since the mGT operates now at constant power output, rather than increasing the generated power by increasing the amount of injected water, now the rotational speed is reducing with this increasing amount due to the action of the controller (Figure 5 (a)). The reduction in rotational speed is only function of the injected water amount at a specific power output and is independent of the saturator performance (Figure 5 (a)), since TIT is kept constant by the control system. The maximal amount of water that can be injected is determined by the surge limit. Due to the reducing rotation speed, at constant power output, the maximal amount is limited to 117 g/s (comparable amount that was found with the second law analysis, 123 g/s [14]).

When looking at the electric efficiency at constant power output, again, a similar trend as at constant rotational speed can be observed (Figure 5): using a constant wet bulb effectiveness of 0.9 does not allow for a sufficient high

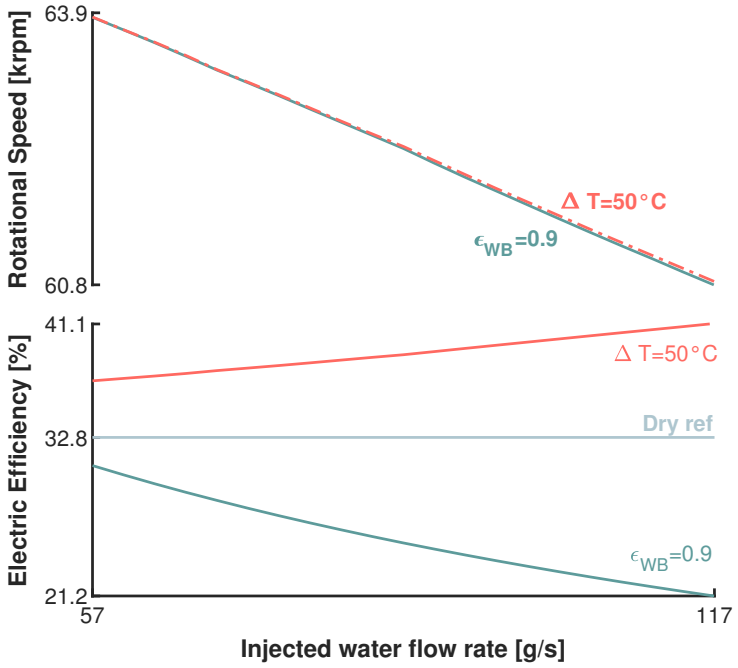

Figure 5: Similar to operation at constant rotational speed, at constant power output (100 kW_e), the performance of the M-power cycle can only be improved by maximizing the waste heat recovery ($\Delta T = 50°C$ case), and while doing so, increasing the electric efficiency.

Table 2: Thermodynamic conditions of the M-power cycle applied on the T100 mGT at each stage of the cycle obtained using Aspen Plus®, for the dry reference case, constant rotational speed ($n = c^{te}$) and constant power output ($P_{gen} = c^{te}$), using constant wet bulb effectiveness ($\epsilon_{\text{WB}} = 0.9$) or constant hot pinch ($\Delta T = 50°C$) at maximal water introduction.

	Dry	**Humid** ($n = c^{te}$)		**Humid** ($P_{gen} = c^{te}$)	
		$\epsilon_{\text{WB}} = 0.9$	$\Delta T = 50°C$	$\epsilon_{\text{WB}} = 0.9$	$\Delta T = 50°C$
Compressor					
T_1 [°C]	15	15	15	15	15
T_2 [°C]	195.4	203.5	203.5	168.2	168.2
p_2 [bar]	4.17	4.34	4.34	3.44	3.44
$\dot{m}_{\text{air}}$ [kg/s]	0.709	0.574	0.574	0.454	0.460
Saturator/Recuperator					
T_3 [°C]	/	64.8	64.8	54.7	54.7
T_4 [°C]	/	93.2	93.0	98.4	98.3
T_5 [°C]	/	104.8	105.7	98.4	98.3
T_6 [°C]	618.8	381.3	646.3	402.0	684.0
T_9 [°C]	262.2	110.7	57.9	108.7	55.3
p_6 [bar]	4.05	4.19	4.19	3.32	3.32
$\dot{m}_{\text{water}}[g/s]$	0	147	153	117	117
ϵ_{dew}	/	0.8	0.8	0.8	0.8
ϵ_{WB}	/	0.9	0.980	0.9	0.975
$\dot{m}_{\text{cond}}$ [g/s]	/	0	99.7	0	80.6
Combustion chamber					
T_7 [°C]	950	950	950	950	950

Table 2: (continued)

	Dry	**Humid** ($n = c^{te}$)		**Humid** ($P_{gen} = c^{te}$)	
		$\epsilon_{\mathrm{WB}} = 0.9$	$\Delta T = 50°C$	$\epsilon_{\mathrm{WB}} = 0.9$	$\Delta T = 50°C$
p_7 [bar]	3.85	3.98	3.98	3.15	3.15
$\dot{m}_{\mathrm{fuel}}$ [g/s]	6.10	12.3	6.93	9.43	4.86
Turbine					
T_8 [°C]	668.8	700.0	696.3	739.2	734.6
p_8 [bar]	1.05	1.05	1.05	1.05	1.05
$\dot{m}_{\mathrm{turb}}$ [kg/s]	0.716	0.733	0.734	0.580	0.582
General					
P_{el} [$\mathrm{kW_e}$]	100.0	144.7	146.1	100.0	100.0
η_{el} [%][2]	32.8	23.6	42.1	21.2	41.1

waste heat recovery to increase the electric efficiency. Similar as at constant rotational speed, the electric efficiency is lower than the dry reference mGT efficiency (32.8%). To improve the performance, a hot pinch of 50°C must be applied to sufficiently reduce the stack temperature (down to 55.3°C) to enable the recovery of the latent heat. By applying this hot pinch the electric efficiency can be increased up to 41.1% (8.9%point absolute increase) which is again close to the limit found using the second law analysis (41.7%) [17].

[2]Reported efficiencies are defined as $\frac{P_{\mathrm{gen}}}{\dot{m}_{\mathrm{fuel}} \mathrm{LHV}}$, not including the losses to the auxiliaries, e.g. pump, cooling fans and fuel compressor, as is the case in the Turbec T100 series 2 engine [33].

However, to achieve this limit, a wet bulb effectiveness of 97.6% is needed, leading to the same technological challenges as mentioned before.

A complete overview of the thermodynamic conditions at the different stages in the M-power cycle is also added for operation at constant power output (100kW$_e$) and at maxiaml water introduction of 117 g/s to Table 2, showing again the main difference between operating at constant wet bulb effectiveness and constant hot pinch: the significant difference in cold outlet temperature of the saturator (402.0°C versus 684.0°C), explaining the very large difference in electrical performance. Finally, the authors would like to draw the attention on the compressor outlet pressure: due to the significant reduction in rotational speed to keep power output constant, the final outlet pressure is reduced significantly from 4.05 bar (dry mGT) to only 3.32 bar (Table 2).

3.2. Technical limitations

Introducing water in the mGT cycle has a significant impact on the mGT components. As previously highlighted by the lead author of this paper [15], this impact includes:

- Turbo-machinery off-design behavior;
- cycle layout limitations;
- combustion stability;
- material and recuperator constraints.

Below, only the specific limitations that apply to the M-power cycle are discussed. For a complete and in-depth discussion, we refer the reader to [15].

For the turbo-machinery, especially surge margin reduction is important. Since the turbine is close to or choked, the total cycle mass flow rate can be considered as rather constant (see Equation 1). An increase in introduced water amount leads automatically to a reduced air amount and thus a shift in compressor operating point. Depending on the operating mode (constant rotational speed or constant power), this shift in operating point is different. However, in both cases, the Surge Margin (SM) is reduced (Figure 6), until finally, the compressor is pushed into surge. Since in this paper, we focused on the thermodynamic aspects, we opted to optimize theoretically the mGT performance, meaning that the results from Table 2 correspond indeed to a SM = 0, with SM defined as:

$$\mathrm{SM}\,(\%) = \left.\frac{\dot{m}_{\mathrm{comp,surge}} - \dot{m}_{\mathrm{comp,working}}}{\dot{m}_{\mathrm{comp,working}}}\right|_{N=cte} \cdot 100\% \tag{5}$$

where $\dot{m}_{\mathrm{comp,working}}$ is the mass flow rate at the current operating point and $\dot{m}_{\mathrm{comp,surge}}$ is the air flow rate through the compressor at the surge limit for the same compressor speed [36]. The use of a 0% SM is from a technical point of view not feasible and requires thus a redesign of the compressor, able of handling the reduced air mass flow rate. In case the original T100 compressor would still be used, a minimal SM must be respected, lowering the maximal amount of water that can be injected. Respecting a SM = 10%, would limit the water injection to 90 g/s at constant rotational speed mode and constant hot pinch of 50°C. This injection leads to a reduced electrical power output of 127.5 $\mathrm{kW_e}$, with a corresponding electric efficiency of 38.7%. At constant power output mode, only 81 g/s of water could be injected, leading to an electric efficiency of 38.5%.

For the material constraints, 2 issues can be identified: increased TOT

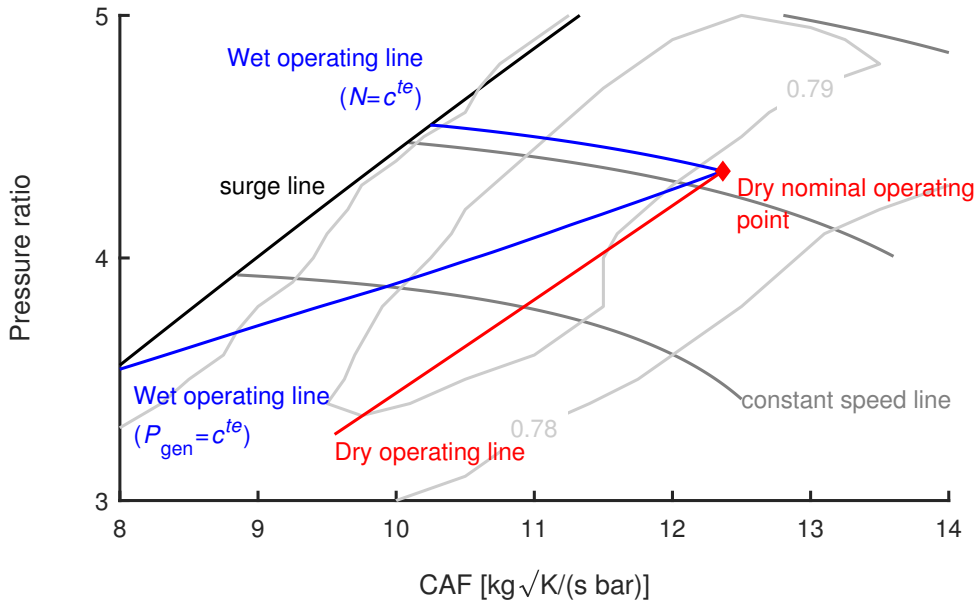

Figure 6: Due to the choking of the turbine, the operation point of the compressor shifts towards the surge limit with increasing water injection (adapted from [15]).

at constant TIT and condensation of water on the hot side of the upper part of the M-power saturator. Current mGTs use as upper temperature limit for the recuperator hot side inlet 650°C (or even 645°C in the case of the Turbec T100 [33]), hence limit for TOT, to avoid the use of more expensive materials. In dry operation in the Turbec T100, a TOT of 645°C corresponds to a TIT of 950°C, which is the limit for an all metallic turbine, hence the limit for TIT. Injecting water in the mGT cycle typically leads to a significant increase of the turbine working fluid heat capacity. This has an impact on the temperature reduction over the turbine during the expansion of the hot gases. Keeping TIT constant while increasing the amount of introduced water, as is the case in this paper, leads to a higher TOT and thus requires the use of better/more expensive materials for the M-power saturator. Lowering the TIT and by doing so, keeping TOT below the limit of 650°C offers a solution. Nevertheless, a lower TIT has a significant negative impact on the electrical performance of the mGT. Indeed, operation at maximal water injection amount of 153 g/s (see Table 2), but with TOT equal to 645°C reduces the electrical power output and efficiency to 137.8 kW_e and 40.6 % (at constant rotational speed) and the efficiency to 38.6% (at constant power output). On the other hand, the lower TOT has a positive effect on the maximal amount of water that can be injected. Indeed, for operation at constant rotational speed, a maximal of 174 g/s of water can be injected before compressor surge is reached, corresponding to an electrical power output of 143.8 kW_e and 41.8% electric efficiency, which is not so far from the performance at constant TIT, but still slightly lower. For operation at constant power output, this effect is even larger: the maximal amount of water that

can be injected increases to 150 g/s with a corresponding efficiency of 40.7%. Since the aim of this paper was to study the thermodynamic potential of the M-power cycle, we still opted to work at constant TIT. Nevertheless, during the design process of the actual M-power saturator, which is not in the scope of this paper, this aspect should be kept in mind.

Apart from the risk of operation at constant TIT to exceed the maximal temperature limit for the M-power saturator, there is no risk to damage this saturator linked with injecting a too limited amount of water or even no water in the real application. In a real application, the heat exchange will just stop as soon as there is no temperature difference. Even when no water is injected, there is no risk in damaging the component, since the temperatures will never exceed the temperatures of the flue gases exiting the turbine (so TOT). Nevertheless, using the M-power saturator in dry conditions makes no sense, since in that case, the lower part will not give any contribution to heat recovery (since no water is injected, the hot compressor air entering will not be cooled down), only leading to additional pressure losses.

A final point of attention from the material point of view is the risk for corrosion. Unlike classical mGTs, where the flue gases exist the machine above the dew point, in the case of the M-power cycle, given the considerable amount of waste heat recovered, the temperature of the flue gases drops below the dew point. This leads to a significant amount of condensed water on the hot side of the M-power saturator (Table 2), which can cause corrosion problems. Since in the M-power saturator, on both sides of the heat exchanger, an air/water or flue gas/water mixture passes, the entire heat exchanger needs to be constructed out of stainless steel to protect against

corrosion. The condensate itself should be eliminated at the bottom of the hot side of the upper part using a drain.

3.3. Sensitivity analysis

To better understand the functioning of the M-power saturator and its impact on the mGT cycle, a sensitivity analysis was performed on several performance parameters of the saturator (ϵ_{WB} and ϵ_{dew}), control parameters (air split fraction, injected water distribution and requested power output), and the inlet conditions (T_{in} and ϕ_{in}). All simulation results presented in this section are obtained using the input parameters from Table 1 and using either $\epsilon_{\mathrm{WB}} = 0.9$ (unless when studying the impact of this value) or using the constant hot pinch of $\Delta T = 50°C$. Moreover, all simulations are performed at constant rotational speed (except when studying the impact of the requested power output), rather than at constant power output, for time savings. Indeed, the additional control loop to change the rotational speed to obtain a constant power output adds a significant extra time to finalize the calculation in Aspen Plus® and leads to some numerical instabilities. Nevertheless, the obtained results at constant generated power output will show similar trends as those presented here, at constant rotational speed.

The first parameter that was varied, the wet bulb effectiveness ϵ_{WB} (ranging from 0.7 to 0.95 with steps of 0.05 and finally with 0.01 until 0.98), shows to have, as already presented before, a significant impact on the electric performance of the mGT (Figure 7). Indeed, a high ϵ_{WB} leads to a much lower stack temperature (see Figure 4), leading to higher waste heat recovery and thus to a higher electric efficiency. A similar observation was made by Alsharif et al. when analyzing the performance of the M-power cycle applied

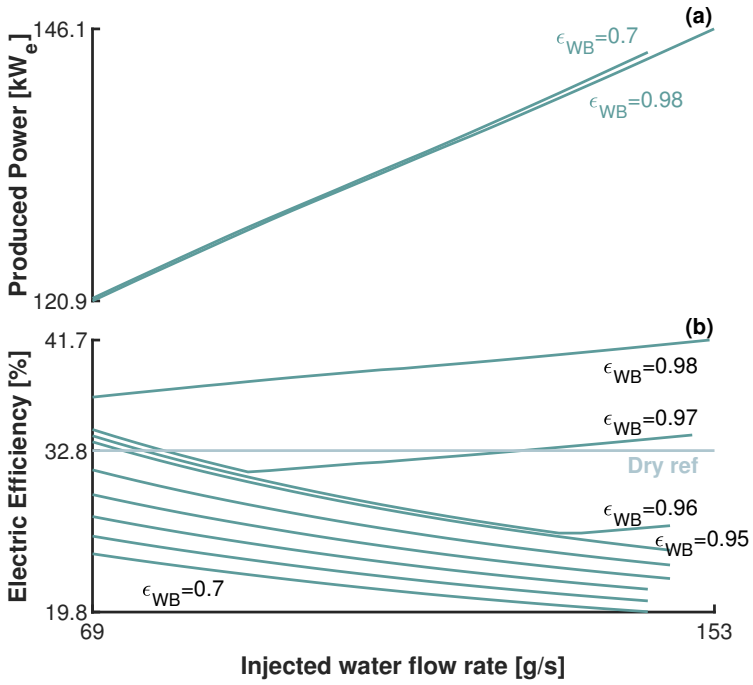

Figure 7: The wet bulb effectiveness ϵ_{WB} has no impact on the produced power. This power is only function of the introduced water amount (a); however, ϵ_{WB} has a large impact on the electric efficiency (b). Increasing the wet bulb effectiveness leads to higher electric efficiency, but at least 98% is needed to reach the dew point of the flue gas to recover the evaporation heat, leading to higher electric efficiency than the dry case (32.8%).

on a larger GT [22]. Produced power is, on the other hand, not affected (Figure 7 (a)), since this parameter only depends on the amount of injected water and not on the quantity of recovered waste heat: a higher waste heat recovery only leads to lower fuel consumption, but no power increase. As presented in subsection 3.1, a ϵ_{WB} of at least 98% is needed to obtain a hot pinch of 50°C (Table 2) and the corresponding increasing electric efficiency with increasing water amount. Indeed, this trend can only be observed at a $\epsilon_{\mathrm{WB}} = 0.98$ and partially at 0.97 and 0.96, although here the recovery is too limited, still leading to a lower electric efficiency compared to the dry reference case (Figure 7 (b)). As mentioned before, this effectiveness is needed to lower the stack temperature sufficiently to start condensing the flue gases and while doing so, liberating and recovering part of the latent heat, which is needed to lead to significant high electric performance increase. It is remarkable to see that only a minor variation in this wet bulb effectiveness can lead to a drastic reduction in performance, going from a significant efficiency increase compared to the dry cycle to similar performance (when going from 0.98 to 0.97) or even to a reduced efficiency (when dropping down to 0.96). Hence, it is strongly required to have a saturator design that is insensitive to possible variations inherent to construction processes, calling thus for a so-called *Robust Design*. This optimization also needs to include a cost analysis to properly assess the thermo-economic potential of the M-power cycle applied to the mGT. To obtain a high ϵ_{WB}, most likely, a larger saturator is need. Hence, a trade-off between cycle performance increase and installation cost needs to be found. Since in this paper, we only focus on the thermodynamic analysis of the cycle, such an analysis was outside the scope of our

paper.

The second saturator performance parameter, ϵ_{dew} (varied from 0.7 to 0.99 in steps of 0.05), has only a small impact on the electric efficiency when working with a constant wet bulb effectiveness ϵ_{WB} and no impact at all when using a constant hot pinch $\Delta T = 50°C$ (Figure 8 (b)). Moreover, similar to ϵ_{WB}, ϵ_{dew} has also no impact at all on the electric output (Figure 8 (a)), for the same reason as mentioned in previous paragraph. At constant ϵ_{WB}, there is thus only a slight positive effect on the electrical efficiency by increasing the ϵ_{dew}. Indeed, a higher ϵ_{dew} leads to a lower hot side outlet temperature of the lower part of the saturator, T_3. This lower T_3 leads then, on its turn, also to a lower $T_{\text{WB},3}$; hence a lower T_9 (see Equation 4). In this case, more waste heat is recovered and thus a higher electrical performance is obtained. This effect is very limited (a minimal efficiency increase of 0.6%points absolute when increasing ϵ_{dew} from 0.7 to 0.99 at the maximum injection of 147 g/s) and overall, the performance is still lower than the performance obtained when keeping the hot pinch constant, $\Delta T = 50°C$, and even lower than the dry performance (32.8%). When using a constant hot pinch, $\Delta T = 50°C$, changing ϵ_{dew} has no impact on the cycle performance. A higher ϵ_{dew} will lead to more heat recovery in the lower part of the saturator from the hot compressed air. However, this has a negative effect on the cold inlet of the upper part. Hence, more heat is exchanged in the first section of the upper part (between (3) and (5) from Figure 1). Since $\Delta T = 50°C$ is constant, a fixed amount of heat is recovered from the flue gases, so less heat is exchanged in the second part (between (5) and (6) from Figure 1). Whether more heat is exchanged in the lower or upper part, has thus no impact at all, since the

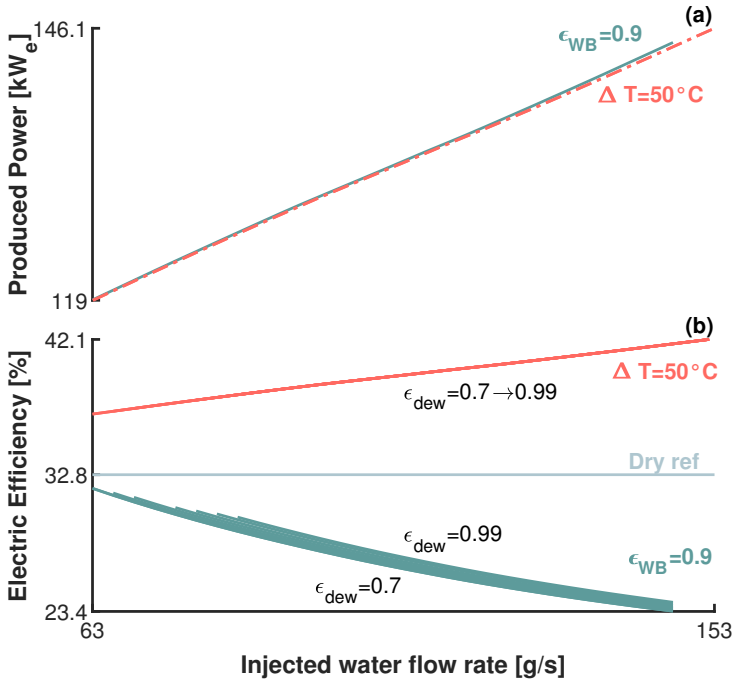

Figure 8: The dew point effectiveness ϵ_{dew} has no impact on the electrical power output, nor on the electric efficiency when assuming a constant hot pinch (case $\Delta T = 50°C$). When working with a constant wet bulb effectiveness (case $\epsilon_{\text{WB}} = 0.9$), a small positive impact can be noticed due to the slight increased heat recovery in the lower part of the M-power saturator.

global amount remains constant. A final observation that can be made, is that the minimal water amount increases with increasing ϵ_{dew} to respect a minimal pinch of 15°C in the lower part of the saturator. This increasing amount is logical, since with increasing ϵ_{dew}, the heat exchange in the lower part is rising. While doing so, T_4 is increasing and thus reducing the hot pinch.

When looking to the impact of the cycle inlet parameters, it is clear to observe that the inlet temperature has a strong negative impact on both electric

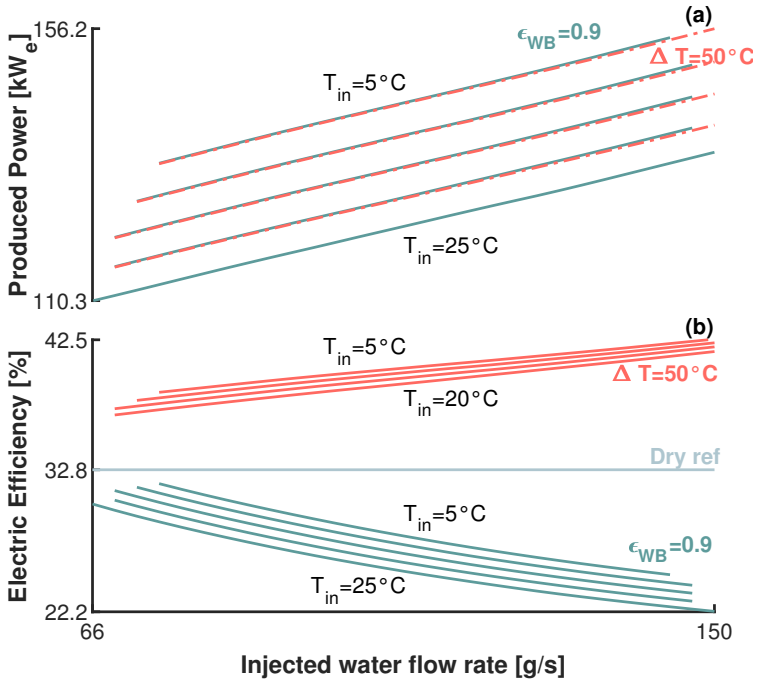

Figure 9: Similar to the dry mGT, the M-power cycle performance is negatively affected by the higher compressor inlet air temperature, due to the worse compressor performance.

power output and efficiency (at both constant ϵ_{WB} and $\Delta T = 50°C$, inlet air temperature varied from 5°C to 25°C, Figure 9). For both cases, this lower cycle performance at higher compressor inlet air temperature, T_1, is mainly due to the compressor performance and less to the saturator performance. As it is generally known, higher inlet temperature leads to a higher compressor power consumption at constant rotational speed (and also a slightly higher compressor outlet temperature) [37]. The higher compressor outlet temperature T_2 leads to a higher outlet temperature of the cold side of the lower part of the saturator T_3 given the constant ϵ_{dew}. Therefore, less waste heat can be recovered. For $\Delta T = 50°C$, this effect is less present, since, as mentioned before, the total amount of heat recovered from the flue gases is fixed (given the constant hot pinch). In that case, the difference in electrical performance is only a result of the higher compressor power. This is reflected in the mean relative efficiency penalty for increasing the inlet air temperature by 5°C: at constant wet bulb effectiveness, the efficiency reduces by 2.9% relatively, while at constant hot pinch, only a relative penalty of 0.6% can be observed. One of the advantages of humidified cycles, highlighted by Jonsson and Yan, was the reduced sensitivity of their performance for changing inlet conditions [6]. For the M-power cycle applied on the mGT, we make a similar observation, since for the dry cycle, increasing the inlet air temperature by 5°C leads to an average penalty of 1.8%, which is significantly higher than the 0.6% of the optimal M-power case (case $\Delta T = 50°C$).

The inlet air humidity ϕ_{in} (varied from 20% to 100% in steps of 20%) is expected to have some impact on the electrical performance, since it impacts T_{dew3} and $T_{\text{WB,3}}$. Indeed, a higher inlet humidity will lead to higher T_{dew3}

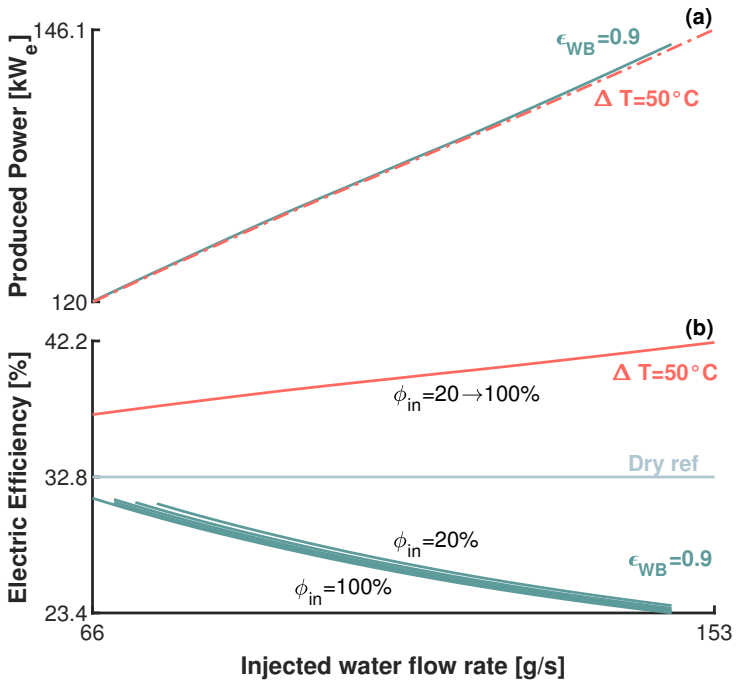

Figure 10: The relative humidity ϕ_{in} of the compressor inlet air has no impact on the global produced power and only a minor negative effect on the electric efficiency when assuming a constant wet bulb effectiveness (case $\epsilon_{\mathrm{WB}} = 0.9$). When using a constant hot pinch (case $\Delta T = 50°C$), the humidity has no impact on the electric efficiency.

and $T_{\mathrm{WB},3}$, leading thus to less waste heat recovery (see Equation 3 and Equation 4). However, the impact on the electric efficiency remains rather limited (Figure 10 (b), case $\epsilon_{\mathrm{WB}} = 0.9$), while there is no noticeable difference on the produced power (Figure 10 (a)). Again, the reason can be found in the higher temperature after the compressor. Even at $\phi_{\mathrm{in}} = 100\%$, the relative humidity after the compressor and saturator is still rather limited ($\phi_3 = 21.4\%$), having thus only a moderate impact on $T_{\mathrm{WB},3}$ (increase from 35.3°C at $\phi_{\mathrm{in}} = 20\%$ to 50.9°C at $\phi_{\mathrm{in}} = 100\%$) and on $T_{\mathrm{dew},3}$ (increase from 12.3°C to 39.4°C). Moreover, at $\Delta T = 50°C$, there is no real impact, since as explained before, a change in T_3 (Equation 3) has only a minor impact on the performance and there is no effect of the changing $T_{\mathrm{WB},3}$ on the heat recovery from the flue gases, given the operation at constant hot pinch. Finally, a higher relative humidity ϕ_{in} has no noticeable impact on the maximal amount of water that can be introduced in the cycle. Indeed, even ϕ_{in} of 100% (full saturation) still corresponds only to an initial water amount in the inlet of 6 g/s, which is negligible compared to the final total amount of injected water of 147 g/s (case $\epsilon_{\mathrm{WB}} = 0.9$) and 153 g/s (case $\Delta T = 50°C$). There is however a minor influence on the minimal amount that needs to be injected in the $\epsilon_{\mathrm{WB}} = 0.9$ case (Figure 10 (b)), due to the better performance of the lower part at higher inlet humidity.

Moreover, simulations showed that both control parameters, air split ratio and water injection division, have no impact at all on the global electric performance of the mGT (Figure 11 and Figure 12). In a first step, the air split ratio was varied from 1/4 in the lower part and 3/4 in the upper part to finally 3/4 and 1/4 respectively, while dividing the water proportionally

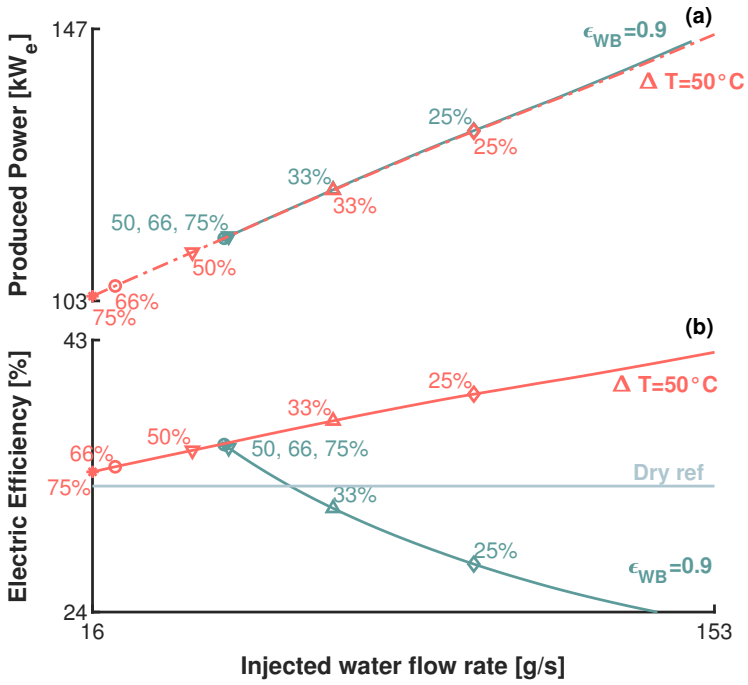

Figure 11: Changing the air split ratio between the lower and upper part of the M-power saturator has no impact on the global performance (produced power (a) and electric efficiency (b)). However, it has a huge impact on the minimal amount of water that needs to be injected to avoid violation of the second law in the lower part (minimal water amounts are indicated for the different split ratios using the markers).

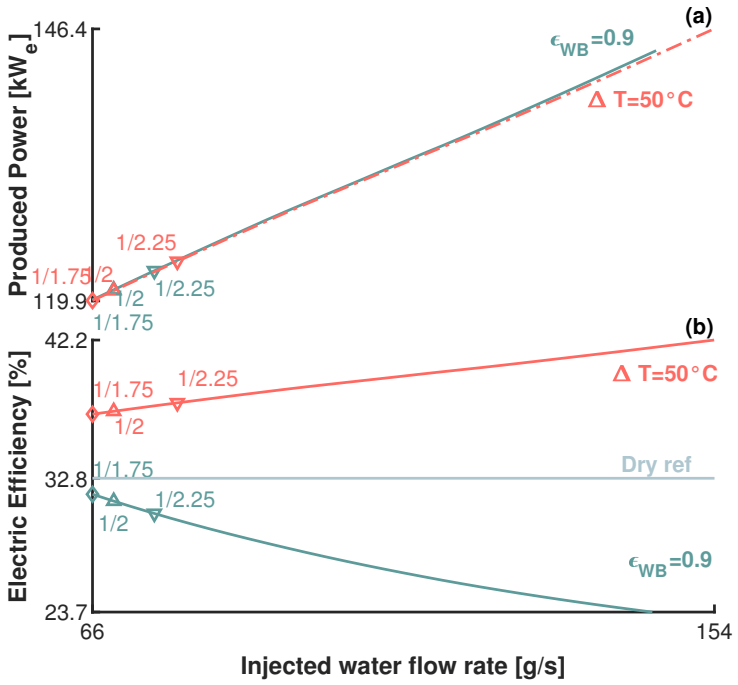

Figure 12: Changing the water division ratio between the lower and upper part of the M-power saturator (ranging from 1/1.75 over 1/2 to 1/2.25) has no effect on the global performance (produced power (a) and electric efficiency (b)). However, it has an impact on the violation of the second law in the lower part (minimal water amounts are indicated for the different division ratios using the markers).

to the air mass flow rate, as is the case in the original setup (Figure 11). Secondly, to study the impact of the water division, the air split fraction was kept constant (1/3 in the lower part and 2/3 in the upper part), but here, the proportion of the introduced water was changed (1/1.75, 1/2 and 1/2.25, Figure 12). As presented in Figure 11 and Figure 12, there is no difference between the different cases in terms of performance. This shows that both control variables have no impact on the global cycle performance. Indeed, in the approach used for the simulations presented in this paper, the performance is calculated based on global energy balances: Equation 3 determines the outlet temperature of the cold stream of the lower part T_3. Passing more or less air (with more or less water present) on the cold side of this lower part, will not change the total amount that is exchanged (in the actual heat exchangers, this will have an influence, since the flow rates will determine the heat exchange coefficients and thus the total amount of exchanged air). A similar comment can be made for the upper part, since the heat exchanged in the upper part depends only on one single temperature: either $T_{\mathrm{WB},3}$ (case $\epsilon_{\mathrm{WB}} = 0.9$) or TOT (case $\Delta T = 50°C$). Both temperatures remain constant for the same input variables and are thus not affected by the control. Although the air flow split and the division of the water amount has thus no impact on the performance, given the use of the global energy balance to calculate the total exchanged heat, at least a minimal air mass flow rate (with a minimal water content) needs to be introduced in both the upper and lower part, to avoid too high outlet temperatures and thus violation of the second law: e.g. by introducing more air in the lower part of the heat exchanger, the lower limited for the water injection can be reduced.

Indeed, a higher fraction passing in this lower part will lead to a pinch larger than 15°C at lower injection rates: e.g. lower limit shifts from 100 g/s for a split fraction of 25% to 16 g/s for a split fraction of 75% (indicated by the different markers on Figure 11 and Figure 12). Finally, again, in the actual case, similarly as for the lower part, changing the air flow rate (and the water fraction) will determine the heat exchange coefficients and thus the actual performance of the saturator. This should be studied in detail when a real design is presented, possibly with consideration of the uncertainties on the design and operational parameters.

Finally, reducing the requested power output has a distinct different behavior when using a constant wet bulb effectiveness of 0.9 or a constant hot pinch, that allows for more waste heat recovery but requires a higher wet bulb effectiveness and thus a better performing saturator (Figure 13). When using a wet bulb effectiveness $\epsilon_{\mathrm{WB}} = 0.9$ operation at part load for a certain constant injection amount leads to lower electric efficiency. Indeed, a lower power output is achieved by lowering the rotational speed and thus also lowering the corresponding air mass flow rate going through the cycle. Hence, at part load, the relative water fraction is higher. The fixed wet bulb effectiveness does not allow to recover more heat (and especially no latent heat) and thus requiring more fuel. On the other hand, using a constant hot pinch leads to similar performance improvements for nominal (100 $\mathrm{kW_e}$) and part load (90 and 80 $\mathrm{kW_e}$), with as only difference a reduced minimal and maximal amount of water due to the lower rotational speed and thus lower air mass flow rates (different symbols indicated maximal and minimal amount in Figure 13). Indeed, a constant hot pinch leads to similar heat

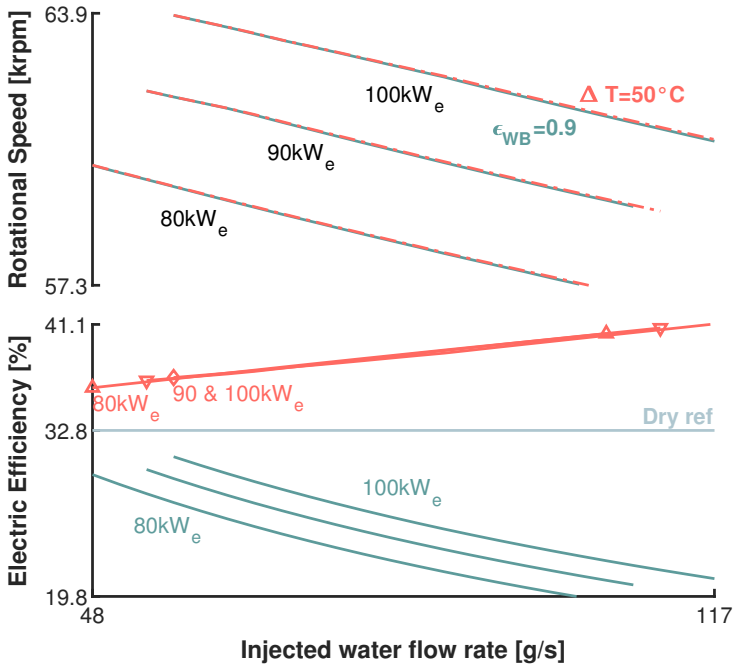

Figure 13: The requested power output has no impact on the global electric performance, when assuming a constant hot pinch ($\Delta T = 50°C$).

recovery for all cases and thus similar performance.

3.4. Exergetic analysis

In an attempt to explain the high potential of the M-power cycle, an exergetic analysis of the cycle, represented using a Grassmann diagram, was performed. For this analysis, the cycle was considered operating at constant nominal power output (100 kW_e) using a constant hot pinch ($\Delta T = 50°C$). Moreover, the exergy analysis was performed following the same procedure as presented by the authors of this paper in [38]. The exergy content of the different flows was obtained using the *EXERGYFL* property implemented in Aspen Plus® while taking 15°C, 1.013 bar and H_2O_{liquid} as dead state. Since

this property only considers thermal exergy, the chemical exergy of the fuel was calculated using formation enthalpy [12].

The Grassmann diagrams shows clearly the major advantages of the M-power cycle: the specific water introduction method together with the aftercooling (Figure 14). In more traditional humidified cycles, e.g. the REVAP® and mHAT cycle, the total water amount is injected after the aftercooler (REVAP®) or after the compressor (mHAT, where no aftercooler is present) in the compressed air and is then evaporated in a heat exchanger. While in the M-power cycle, the water is injected and evaporates gradually in one singe component. Using direct injection of the total stream leads to a considerable exergy destruction, due to the temperature difference between compressed air and cold water and the sudden full injection: e.g. in the mHAT cycle operating at nominal power output of 100 kW_e, 14 kW exergy is destructed in the saturator [38]. Although this local destruction leads later to a larger recovery in the recuperator (198 kW versus 168 kW in the dry cycle [38]), due to the lower inlet temperature, the exergy is lost, explaining the lower performance. By applying the specific introduction method in the M-power cycle, this exergy destruction could be avoided. In the M-power cycle, only a very small fraction of the total exergy flow in the cycle is lost in the aftercooler (6 kW, Figure 14); however, no additional exergy is lost during the water injection and the passage through the cold side of the lower and upper part of the heat exchanger. The action of the aftercooler together with the injection of cold water leads to a significant lower temperature of the compressed air stream, allowing for a very large exergy recovery in the M-power saturator: 36 kW in the first section of the upper part (between points 3 and

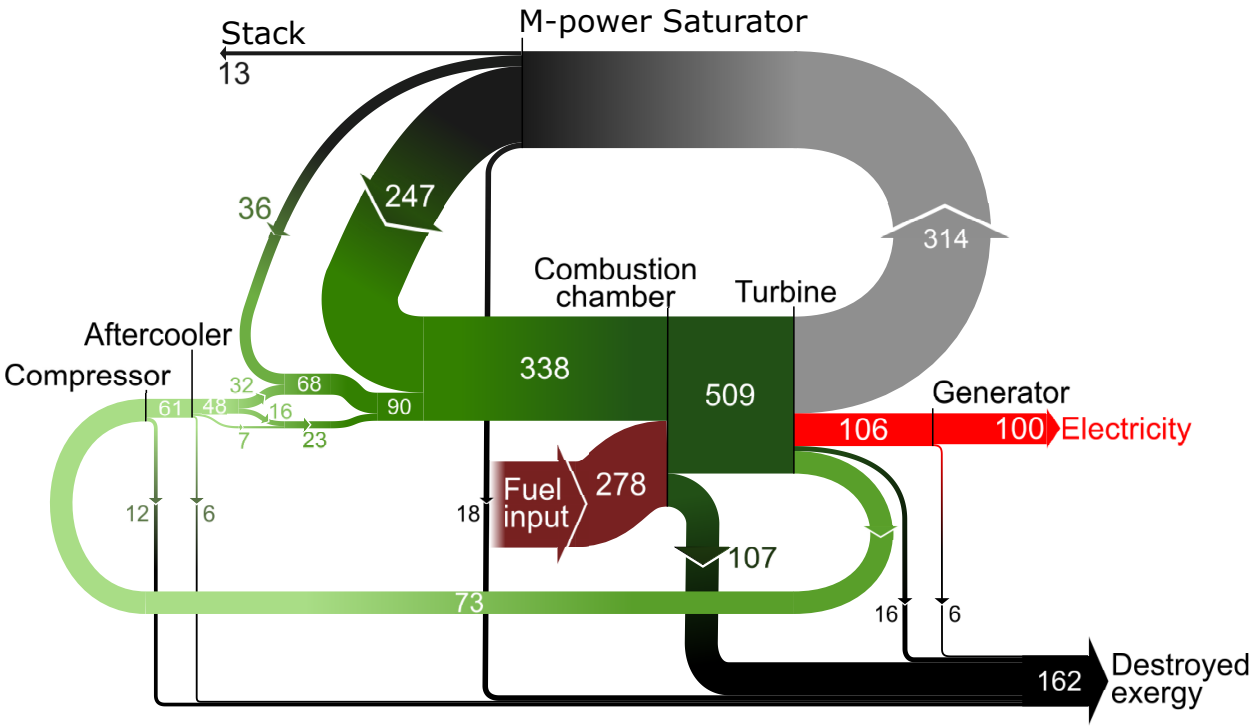

Figure 14: The Grassmann diagram of the M-power cycle applied on the mGT represents the exergy flows (expressed in kW) in the cycle and allows to determine the exergy efficiency (36.0%) of the cycle

5 on Figure 1) and 247 kW in the last section of the upper part (between points 4/5 and 6 on Figure 1). Finally, the M-power saturator displays a total exergy destruction of 8.6%, defined as the ratio between the difference in incoming ($\sum_{\text{in}} \dot{E}x$) and outgoing exergy streams ($\sum_{\text{out}} \dot{E}x$) in the M-power saturator and the exergy input in the global cycle from the fuel ($\dot{E}x_{\text{fuel}}$):

$$BB^{\text{dest}} = \frac{\sum_{\text{in}} \dot{E}x - \sum_{\text{out}} \dot{E}x}{\dot{E}x_{\text{fuel}}}, \tag{6}$$

while the exergy efficiency of the component, defined as the ratio between the sum of the exergy of the streams that gain exergy ($\sum_{\text{gain}} \Delta\dot{E}x$), and the sum of the exergy of the streams that lose exergy ($\sum_{\text{loss}} \Delta\dot{E}x$), achieves 92%:

$$BB^{\text{eff}} = \frac{\sum_{\text{gain}} \Delta\dot{E}x}{\sum_{\text{loss}} \Delta\dot{E}x}. \tag{7}$$

Both values are close to the maximum values set by Bram et al.: 5% destruction and 93% heat exchanger efficiency [12], highlighting again that the performance of the cycle is indeed approaching the thermodynamic limit. Hence, the M-power cycle present a final exergy efficiency of 36.0%, which is significantly higher than the 29.3% electric exergy efficiency of the dry mGT and the 30.6% of the mHAT [38]. Moreover, the exergy efficiency of the M-power cycle even exceeds the dry mGT CHP total exergy efficiency of 35.7%.

4. Conclusion

In this paper, we assessed the performance of the M-power cycle applied on the mGT. An experimentally validated Aspen Plus® model of the Turbec

T100 was converted to the M-power cycle by implementing the specific saturator. Numerical results indicated that the electrical power can be increased when operating at constant rotational speed by water introduction (up to 144.7 kW_e for an injection of 147 g/s). However, when applying a typical dew point effectiveness of 0.9 for the upper part of the M-power saturator, no electric efficiency increase can be achieved. Moreover, a decrease by 9.2%point when operating at constant rotational speed and even 11.6%point at constant power output compared to the dry reference case was observed. Allowing for more waste heat recovery, by increasing this effectiveness (up to 98%, leading to a hot saturator pinch of 50°C) and by doing so, lowering the stack temperature up to the dew point of the flue gases (57°C), leads to a significant electric efficiency increase. Efficiency increases up to the limit found using 2nd law analysis: maximal injection of 153 g/s leads to a 46.1 kW_e power output and 9.3%point absolute efficiency increase at constant rotational speed. At constant power output of 100 kW_e, a maximal amount of 117 g/s could be injected, leading to a slightly lower electric efficiency increase of 8.3%point. The main difficulty remains, however, the 98% dew point effectiveness in the saturator, which can be challenging (or even thermo-economically impossible) to achieve. The sensitivity analysis highlighted that only the compressor inlet air temperature has an impact on the produced power, while inlet air temperature and wet bulb effectiveness have a large impact on the electric efficiency. Inlet air humidity and dew point effectiveness only have a minor impact when operating at constant dew point effectiveness and no impact when operating at a constant hot pinch. The saturator control parameters, being air split ratio and water division over the

lower and upper part of the saturator, have no impact at all on the global cycle performance. Finally, the exergy analysis indicated that the superiority of the M-power cycle is found in the specific water introduction method, that does not lead to extra exergy losses, as is the case in other humidified cycles, leading to an exergy efficiency of up to 36% at constant power output of 100 kW_e.

Future works involve a more in-depth analysis of the saturator by proposing an actual geometry and assessing the impact of changing the inlet conditions and geometry of this saturator on its performance as well as on the global cycle in general.

5. Nomenclature

CHAT	Cascaded Humidified Advanced Turbine
CHP	Combined Heat and Power
EvGT	Evaporative Gas Turbine
GT	Gas Turbine
HAT	Humid Air Turbine
mGT	micro Gas Turbine
mHAT	micro Humid Air Turbine
RE	Renewable Energy
REVAP®	REgenerative EVAPoration
SM	Surge Margin
TIP	Turbine Inlet Pressure

TIT	Turbine Inlet Temperature
TOPHAT®	TOP Humid Air Turbine
TOT	Turbine Outlet Temperature

References

[1] Gahleitner, G.. Hydrogen from renewable electricity: An international review of power-to-gas pilot plants for stationary applications. International Journal of Hydrogen Energy 2013;38(5):2039 – 2061.

[2] U.S. Department of Energy, Office of Energy Efficiency & Renewable Energy, Office of Power Technologies, . Advanced microturbine systems – Program plan for fiscal years 2000 through 2006. 2000. Online available: `http://www.energetics.com/resourcecenter/products/plans/samples/Documents/advanced_microturbine_plan.pdf` (accessed: 14-09-2014).

[3] Delattin, F., Bram, S., Knoops, S., De Ruyck, J.. Effects of steam injection on microturbine efficiency and performance. Energy 2008;33(2):241 – 247.

[4] Montero Carrero, M., De Paepe, W., Parente, A., Contino, F.. T100 mGT converted into mHAT for domestic applications: Economic analysis based on hourly demand. Applied Energy 2015;164:1019–1027.

[5] Stathopoulos, P., Paschereit, C.. Retrofitting micro gas turbines for wet operation. a way to increase operational flexibility in distributed CHP plants. Applied Energy 2015;154:438 – 446.

[6] Jonsson, M., Yan, J.. Humidified gas turbines – A review of proposed and implemented cycles. Energy 2005;30(7):1013 – 1078.

[7] Rao, A.D.. Process for producing power. US patent no. 4829763. 1989.

[8] Thern, M.. Humidification processes in gas turbine cycles. Lund University; 2005.

[9] Nakhamkin, M., Swensen, E.C., Wilson, J.M., Gaul, G., Polsky, M.. The Cascaded Humidified Advanced Turbine (CHAT). Journal of Engineering for Gas Turbines and Power 1996;118(3):565–571.

[10] Van Liere, J., Laagland, G.. The TOPHAT® cycle. VDI-Berichte 2000;:161–175.

[11] De Ruyck, J., Bram, S., Allard, G.. REVAP® cycle: A new evaporative cycle without saturation tower. Journal of Engineering for Gas Turbines and Power 1997;119(4):893–897.

[12] Bram, S., De Ruyck, J.. Exergy analysis tools for ASPEN applied to evaporative cycle design. Energy Conversion and Management 1997;38(15-17):1613 – 1624.

[13] Parente, J., Traverso, A., Massardo, A.F.. Micro humid air cycle: Part A – Thermodynamic and technical aspects. In: ASME Conference Proceedings. ASME paper GT2003-38326; 2003, p. 221–229.

[14] De Paepe, W., Montero Carrero, M., Bram, S., Contino, F., Parente, A.. Waste heat recovery optimization in micro gas turbine applications

using advanced humidified gas turbine cycle concepts. Applied Energy 2017;207:218–229.

[15] De Paepe, W., Montero Carrero, M., Bram, S., Parente, A., Contino, F.. Towards higher micro gas turbine efficiency and flexibility — Humidified mGTs: A review. Journal of Engineering for Gas Turbines and Power 2017;140(8):081702.

[16] De Paepe, W., Delattin, F., Bram, S., De Ruyck, J.. Water injection in a micro gas turbine – Assessment of the performance using a black box method. Applied Energy 2013;112:1291–1302.

[17] De Paepe, W., Contino, F., Delattin, F., Bram, S., De Ruyck, J.. Optimal waste heat recovery in micro gas turbine cycles through liquid water injection. Applied Thermal Engineering 2014;70(1):846–856.

[18] Gillan, L., Maisotsenko, V.. Maisotsenko open cycle used for gas turbine power generation. In: ASME Turbo Expo 2003, collocated with the 2003 International Joint Power Generation Conference. American Society of Mechanical Engineers Digital Collection; 2003, p. 75–84.

[19] Sadighi Dizaji, H., Hu, E.J., Chen, L.. A comprehensive review of the maisotsenko-cycle based air conditioning systems. Energy 2018;156:725 – 749.

[20] Wicker, K.. Life below the wet bulb: The maisotsenko cycle. Power 2003;147(9):29.

[21] Reyzin, I.. Evaluation of the maisotsenko power cycle thermodynamic

efficiency. International Journal of Energy for a Clean Environment 2011;12(2-4).

[22] Alsharif, A., Gadalla, M., Dincer, I.. Energy and exergy analysis of maisotsenko cycle. In: ASME 2011 5th international conference on energy sustainability & 9th fuel cell science. 2011, p. 1–7.

[23] Saghafifar, M., Gadalla, M.. Innovative inlet air cooling technology for gas turbine power plants using integrated solid desiccant and maisotsenko cooler. Energy 2015;87:663–677.

[24] Saghafifar, M., Gadalla, M.. Analysis of maisotsenko open gas turbine power cycle with a detailed air saturator model. Applied Energy 2015;149:338–353.

[25] Saghafifar, M., Gadalla, M.. Analysis of maisotsenko open gas turbine bottoming cycle. Applied Thermal Engineering 2015;82:351–359.

[26] Tariq, R., Sheikh, N.A.. Numerical heat transfer analysis of maisotsenko humid air bottoming cycle — a study towards the optimization of the air-water mixture at bottoming turbine inlet. Applied Thermal Engineering 2018;133:49 – 60.

[27] Zhu, G., Chow, T., Fong, K., Lee, C.. Comparative study on humidified gas turbine cycles with different air saturator designs. Applied Energy 2019;254:113592.

[28] De Paepe, W., Montero Carrero, M., Giorgetti, S., Parente, A., Bram, S., Contino, F.. Exhaust gas recirculation on humidified flexible micro

gas turbines for carbon capture applications. In: ASME Conference Proceedings. ASME paper GT2016-57265; 2016, p. V003T06A011.

[29] Montero Carrero, M., De Paepe, W., Magnusson, J., Parente, A., Bram, S., Contino, F.. Experimental characterisation of a micro humid air turbine: assessment of the thermodynamic performance. Applied Thermal Engineering 2017;118:796 – 806.

[30] Renzi, M., Caresana, F., Pelagalli, L., Comodi, G.. Enhancing micro gas turbine performance through fogging technique: Experimental analysis. Applied Energy 2014;135:165 – 173.

[31] Çengel, Y., Boles, M.. Thermodynamics: an engineering approach. McGraw-Hill series in mechanical engineering; Boston, US: McGraw-Hill Higher Education; 2006. ISBN 9780072884951.

[32] De Paepe, W., Renzi, M., Montero Carrerro, M., Caligiuri, C., Contino, F.. Micro gas turbine cycle humidification for increased flexibility: Numerical and experimental validation of different steam injection models. Journal of Engineering for Gas Turbines and Power 2019;141(2).

[33] Turbec AB, . T100 microturbine CHP system: Technical description ver 4.0; 2000-2001.

[34] Pezzini, P., Tucker, D., Traverso, A.. Avoiding compressor surge during emergency shutdown hybrid turbine systems. Journal of Engineering for Gas Turbines and Power 2013;135:102602 (10 pages).

[35] Copeland Corporation, . Copeland scroll fuel gas booster/gas compression package: Installation, operation and maintenance manual. Tech. Rep.; Copeland Corporation; 2002.

[36] Brun, K., Nored, M.G.. GMRC guideline – Release version 4.3: Application guideline for centrifugal compressor surge control systems. Tech. Rep.; Gas Machinery Research Council, Southwest Research Institute; 2008. Online available: `https://www.gmrc.org/documents/GMRCSurgeGuideline_000.pdf` (accessed: 12-09-2014).

[37] Comodi, G., Renzi, M., Caresana, F., Pelagalli, L.. Enhancing micro gas turbine performance in hot climates through inlet air cooling vapour compression technique. Applied Energy 2015;147(0):40 – 48.

[38] Montero Carrero, M., De Paepe, W., Bram, S., Parente, A., Contino, F.. Does humidification improve the micro gas turbine cycle? thermodynamic assessment based on sankey and grassmann diagrams. Applied Energy 2017;204:1163–1171.